



IFIT5 Participates in the Antiviral Mechanisms of Rainbow Trout Red Blood Cells

Veronica Chico^{1,2}, Maria Elizabet Salvador-Mira^{1,2}, Ivan Nombela^{1,2}, Sara Puente-Marin^{1,2}, Sergio Ciordia³, María Carmen Mena³, Luis Perez^{1,2}, Julio Coll⁴, Fanny Guzman⁵, Jose Antonio Encinar^{1,2}, Luis Mercado⁵ and Maria del Mar Ortega-Villaizan^{1,2*}

¹ Departamento de Bioquímica y Biología Molecular, Instituto de Biología Molecular y Celular (IBMC), Universidad Miguel Hernández (UMH), Elche, Spain, ² Departamento de Bioquímica y Biología Molecular, Instituto de Investigación, Desarrollo e Innovación en Biotecnología Sanitaria de Elche (IDIIE), Universidad Miguel Hernández (UMH), Elche, Spain, ³ Unidad de Proteómica, Centro Nacional de Biotecnología (CNB-CSIC), Madrid, Spain, ⁴ Departamento de Biotecnología, Instituto Nacional de Investigaciones y Tecnologías Agrarias y Alimentarias (INIA), Madrid, Spain, ⁵ Grupo de Marcadores Inmunológicos, Laboratorio de Genética e Inmunología Molecular, Instituto de Biología, Pontificia Universidad Católica de Valparaíso (PUCV), Valparaíso, Chile

OPEN ACCESS

Edited by:

Tiehui Wang,
University of Aberdeen,
United Kingdom

Reviewed by:

Kevin R. Maisey,
Universidad de Santiago de Chile,
Chile
Yibing Zhang,
Chinese Academy of Sciences, China
Jun Li,
Lake Superior State University,
United States

*Correspondence:

Maria del Mar Ortega-Villaizan
morteaga-villaizan@umh.es

Specialty section:

This article was submitted to
Comparative Immunology,
a section of the journal
Frontiers in Immunology

Received: 22 October 2018

Accepted: 07 March 2019

Published: 16 April 2019

Citation:

Chico V, Salvador-Mira ME, Nombela I, Puente-Marin S, Ciordia S, Mena MC, Perez L, Coll J, Guzman F, Encinar JA, Mercado L and Ortega-Villaizan MDM (2019) IFIT5 Participates in the Antiviral Mechanisms of Rainbow Trout Red Blood Cells. *Front. Immunol.* 10:613. doi: 10.3389/fimmu.2019.00613

Viral hemorrhagic septicemia virus (VHSV) infection appears to be halted in rainbow trout nucleated red blood cells (RBCs). Diverse mechanisms are thought to be related to the antiviral immune response of rainbow trout RBCs to VHSV. However, the specific rainbow trout RBC proteins that interact directly with VHSV are still unknown. In an attempt to identify VHSV-RBC protein interactions, we characterized the immunoprecipitated (IP) proteome of RBCs exposed to VHSV using an antibody against the N protein of VHSV. The IP proteomic characterization identified 31 proteins by mass spectrometry analysis. Among them, we identified interferon-induced protein with tetratricopeptide repeats 5 (IFIT5), a protein belonging to a family of proteins that are induced after the production of type I interferon. Importantly, IFIT5 has been implicated in the antiviral immune response. We confirmed the participation of IFIT5 in the rainbow trout RBC antiviral response by examining the expression profile of IFIT5 in RBCs after VHSV exposure at transcriptional and protein levels. We detected a correlation between the highest IFIT5 expression levels and the decline in VHSV replication at 6 h post-exposure. In addition, silencing *ifit5* resulted in a significant increase in VHSV replication in RBCs. Moreover, an increase in VHSV replication was observed in RBCs when the IFIT5 RNA-binding pocket cavity was modulated by using a natural compound from the SuperNatural II database. We performed a proximity ligation assay and detected a significant increase in positive cells among VHSV-exposed RBCs compared to unexposed RBCs, indicating protein-protein colocalization between IFIT5 and the glycoprotein G of VHSV. In summary, these results suggest a possible role of IFIT5 in the antiviral response of RBCs against VHSV.

Keywords: rainbow trout, IFIT5, red blood cells, erythrocyte, VHSV, antiviral immune response, immunoprecipitate, proteomic

INTRODUCTION

The role of nucleated red blood cells (RBCs) as immune response cell mediators has become clearer in recent years. Fish RBCs are the most common cell type in the blood and are best known for their functions in gas exchange and respiration. In mammals, mature RBCs are oval, biconcave cells that lack nuclei, organelles, and ribosomes (1). In non-mammalian vertebrates, RBCs are oval, flattened, biconvex disks with a nucleus and organelles in their cytoplasm (2), allowing them to *de novo* synthesize molecules in response to stimuli. Indeed, a set of biological processes related to antiviral immunity has been described in nucleated RBCs (3).

Recent studies have demonstrated that RBCs halt viral hemorrhagic septicemia rhabdovirus (VHSV) infection (4). The virus enters the cell, but does not replicate at levels comparable to piscine orthoreovirus or infectious salmon anemia virus (ISAV) infections in salmon RBCs (5, 6). Several mechanisms have been suggested to be involved in the antiviral response of rainbow trout RBCs to VHSV, such as increased protein levels of β -defensin 1 (BD1, an antimicrobial peptide involved in antiviral innate immunity), global protein synthesis inhibition corresponding to a virus and host cell shut-off, or an antioxidant-related antiviral response (4). Further, an increase in the expression of IFN-related genes and proteins, such as Mx, has been observed in infectious pancreatic necrosis virus-exposed RBCs, where the viral infection was also non-productive (7).

Interferon-induced proteins with tetratricopeptide repeats (IFIT) are a family of proteins that are strongly induced after the production of type I interferon (8). The IFIT family is conserved in mammals, amphibians, birds, and bony fishes, but is not present in yeast, plants, or invertebrates (8). IFIT genes have been identified for many mammal species, as well as for various birds, reptiles, amphibians, and bony fishes. The number of IFIT genes and the composition of the family varies greatly between species (9). Knowledge of IFIT genes is scarce in teleost species compared to humans. Recently, the complete repertoire of IFIT genes was described in zebrafish (10). IFIT proteins contain repeats of tetratricopeptide (TPR domains) and mediate a wide variety of protein-protein and RNA-protein interactions involved in the initiation of translation, virus replication, double-stranded RNA signaling, cell migration, and proliferation (11, 12). The multiple TPR domains may allow IFIT proteins to participate in the regulation of viral gene transcription and translation and in the negative regulation of the host inflammatory and antiviral response (12, 13). Recently, it has been shown that members of the IFIT family selectively restrict viral replication by recognition of viral mRNA via binding of 2'-O methylated RNA or 5'-triphosphate RNA (14–16). Other studies have found that members of the IFIT family decreased host cap-dependent protein translation by binding to the subunits of the eukaryotic initiation factor 3 (eIF3) translation complex (17). Studies conducted using double hybrid technique (Y2H) also suggested that IFIT proteins could bind to other viral proteins. For example, IFIT1 has been described to bind E1, a viral helicase of human papilloma virus (HPV) required for replication, sequestering it

within the cytoplasm and preventing viral replication in the nucleus (18).

In an attempt to elucidate the molecules responsible for halting VHSV replication inside rainbow trout RBCs, we characterized the RBC proteome that immunoprecipitates with the N protein of VHSV after RBC exposure to the virus. The IFIT5 protein was identified, and additional experiments confirmed the participation of IFIT5 in the rainbow trout RBC antiviral response. We determined the expression profile of IFIT5 in VHSV-exposed RBCs and detected a correlation between the highest IFIT5 expression level and diminished VHSV replication at 6 h post exposure (hpe) to VHSV. In addition, silencing *ifit5* resulted in a significant increase in VHSV replication in RBCs. IFIT5 modulation activity assays were performed by modulating the IFIT5 RNA-binding pocket cavity using a natural compound from the SuperNatural II (19) database identified through a molecular docking procedure. VHSV replication increased in VHSV-exposed RBCs when the IFIT5 RNA-binding pocket cavity was modulated by the compound. Moreover, a proximity ligation assay (PLA) was performed to investigate possible protein-protein colocalization between IFIT5 and the glycoprotein G of VHSV (GVHSV). A significant increase in positive cells was detected among VHSV-exposed RBCs compared with unexposed RBCs. Altogether, the results support a potential role of IFIT5 in the antiviral response of RBCs against VHSV.

MATERIALS AND METHODS

Animals

Rainbow trout (*Oncorhynchus mykiss*) >6 to 7 cm were obtained from Pizolla S.L., Cimballa Fish Farm, (Zaragoza, Spain) and maintained at the University Miguel Hernandez (UMH) facilities at 14°C. Before experimentation, fish were acclimatized to laboratory conditions for 2 weeks. All experimental protocols were reviewed and approved by the Animal Welfare Body and the Research Ethics Committee at the UMH and by the competent authority of the Regional Ministry of Presidency and Agriculture, Fisheries, Food and Water supply. Animal care and all activities involving animal handling and experiments were done according to Spanish [Real Decreto 1201/2005] and EU [EU Directive EC86/609, and Appendix A to Convention ETS123, 2007/526/CE] regulations and recommendations for animal experimentation.

Cell Cultures and Virus

Rainbow trout RBCs were obtained and purified as previously described (4, 7). Briefly, RBCs extracted from the caudal vein were purified by 2 successive Ficoll density gradient centrifugations (7,206 g, Ficoll 1.007; Sigma-Aldrich, Madrid, Spain). Ficoll-purified RBCs were maintained in 25 cm² flasks (Nunc Roskilde, Denmark) with RPMI-1640 medium (Dutch modification) (Gibco, Thermo Fisher Scientific, Carlsbad, CA) supplemented with 10% fetal bovine serum (FBS) gamma irradiated (Cultek, Madrid, Spain), 1 mM pyruvate (Gibco), 2 mM L-glutamine (Gibco), 50 μ g/mL gentamicin (Gibco),

2 µg/mL fungizone (Gibco), 100 U/mL penicillin (Sigma-Aldrich), and 100 µg/mL streptomycin (Sigma-Aldrich) at 14°C for 24 h prior to experimentation.

The RTG-2 (rainbow trout gonad-2) cell line was purchased from the American Type Culture Collection (ATCC 50643) and maintained at 21°C in MEM medium (Sigma-Aldrich) containing 10% FBS, 1 mM pyruvate, 2 mM L-glutamine, 50 µg/mL gentamicin, and 2 µg/mL fungizone.

VHSV strain 07.71 (20) was purchased from the American Type Culture Collection (ATCC VR-1388) and cultured in fathead minnow epithelioma papulosum cyprini (EPC) (21) cells at 14°C as previously described (22).

Immunoprecipitation Assay

Ficoll-purified RBCs from 3 fish were exposed to VHSV at multiplicity of infection (MOI) 1 for 3 h as previously described (4). Unexposed RBCs were used as a control. RBCs were washed 3 times with phosphate-buffered saline (PBS), and the pellet was resuspended in RIPA buffer (50 mM Tris-HCl [Sigma-Aldrich] pH 7.4, 150 mM NaCl [Sigma-Aldrich], 1% Triton X-100 [Sigma-Aldrich], 1% sodium deoxycholate [Sigma-Aldrich], 0.1% sodium dodecyl sulfate [SDS; NZY Tech, Genes and Enzymes, Lisbon, Portugal], 1 mM EDTA [Sigma-Aldrich]) with a cocktail of protease inhibitors (Sigma-Aldrich). The cell pellet was homogenized using pestles (Invitrogen, Thermo Fisher Scientific) and kept at −20°C until use. Cell lysate was precleared with 50 µL protein A Sepharose 4 Fast Flow (GE Healthcare, Little Chalfont, UK) for 1 h at 4°C. Samples were centrifuged at 12,000 × g for 20 s, and supernatants were incubated with monoclonal murine 2C9 antibody against N protein of VHSV (23) diluted 1/500 overnight at 4°C. Immune complexes were precipitated by adding 50 µL protein A Sepharose 4 Fast Flow (GE Healthcare) for 1 h at 4°C. After washing the pellet with RIPA buffer, immune complexes were dissociated by heating the samples in 2X loading sample buffer (from 5X loading sample buffer: 0.225 M Tris-Cl [pH 6.8], 50% glycerol [Sigma-Aldrich], 5% SDS, 0.05% bromophenol blue [Panreac, Barcelona, Spain], and 0.25 M dithiothreitol [Invitrogen, Thermo Fisher Scientific]) for 3 min at 95°C. After centrifugation at 12,000 × g for 20 s, we analyzed the supernatant by mass spectrometry.

In-gel Protein Digestion

Each immunoprecipitated sample was eluted with 2X loading sample buffer and then applied into 1.2 cm wide wells of a conventional SDS-PAGE gel (1 mm thick, 4% acrylamide for the stacking gel, and 12% acrylamide for the resolving gel). The run was stopped as soon as the front was 1 cm into the resolving gel, so that the whole proteome was concentrated in the stacking/resolving gel interface. The unseparated protein bands were visualized by Coomassie staining, excised, cut into 1 mm² cubes, deposited in 96 well plates, and processed automatically in a Proteiner DP (Bruker Daltonics, Bremen, Germany). The digestion protocol was based on Schevchenko et al. (24) with minor variations: gel plugs were washed first with 50 mM ammonium bicarbonate and second with ACN prior to reduction with 10 mM DTT in 25 mM ammonium bicarbonate solution,

and alkylation was carried out with 55 mM IAA in 50 mM ammonium bicarbonate solution. Gel pieces were rinsed first with 50 mM ammonium bicarbonate and second with ACN and then were dried under a stream of nitrogen. Proteomics-grade Trypsin (Sigma-Aldrich) at a final concentration of 16 ng/µL in 25% ACN/50 mM ammonium bicarbonate solution was added, and the digestion took place at 37°C for 4 h. The reaction was stopped by adding 50% ACN/0.5% TFA for peptide extraction. The tryptic eluted peptides were dried by speed-vacuum centrifugation and were cleaned/desalted using Stage-Tips with Empore 3M C18 disks (Sigma-Aldrich).

Liquid Chromatography and Mass Spectrometry Analysis

A 1 µg aliquot of each digested sample was subjected to 1D-nano LC ESI-MS/MS analysis using a nano liquid chromatography system (Eksigent Technologies nanoLC Ultra 1D plus, SCIEX, Foster City, CA) coupled to a high-speed Triple TOF 5600 mass spectrometer (SCIEX) with a Nanospray III source. The analytical column was a silica-based, reversed-phase Acquity UPLC[®] M-Class Peptide BEH C18 Column, 75 µm × 150 mm, 1.7 µm particle size, and 130 Å pore size (Waters Corporation, Milford, MA, USA). The trap column was a C18 Acclaim PepMap[™] 100 (Thermo Fisher Scientific), 100 µm × 2 cm, 5 µm particle diameter, 100 Å pore size, switched online with the analytical column. The loading pump delivered a solution of 0.1% formic acid in water at 2 µL/minutes. The nano-pump provided a flow rate of 250 nL/minutes and was operated under gradient elution conditions. Peptides were separated using a 100-min gradient ranging from 2 to 90% mobile phase B (mobile phase A: 2% acetonitrile, 0.1% formic acid; mobile phase B: 100% acetonitrile, 0.1% formic acid). Injection volume was 5 µL.

Data acquisition was performed with a TripleTOF 5600 System (SCIEX). Data were acquired using an ionspray voltage floating (ISVF) 2300 V, curtain gas (CUR) 35, interface heater temperature (IHT) 150, ion source gas 1 (GS1) 25, and declustering potential (DP) 100 V. All data were acquired using information-dependent acquisition (IDA) mode with Analyst TF 1.7 software (SCIEX). For IDA parameters, 0.25 s MS survey scans in the mass range of 350–1,250 Da were followed by 35 MS/MS scans of 100 ms in the mass range of 100–1,800 (total cycle time: 4 s). Switching criteria were set to ions greater than mass-to-charge ratio (m/z) 350 and smaller than m/z 1,250 with charge state of 2–5 and an abundance threshold of >90 counts per second (cps). Former target ions were excluded for 15 s. An IDA rolling collision energy (CE) parameters script was used to automatically control the CE.

Proteomic Data Analysis, Sequence Search, and Protein Network Analysis

Mass spectrometry data obtained were processed using PeakView v2.2 Software (SCIEX) and exported as mgf files that were searched using Mascot Server v2.5.1 (Matrix Science, London, UK) against a protein database including Teleostei protein sequences from Uniprot/Swissprot Knowledgebase (last update:

20170412, 2,542,118 sequences), together with commonly occurring contaminants, as previously described (25).

Search parameters were set as follows: enzyme, trypsin; allowed missed cleavages, 2; and carbamidomethyl (C) as fixed modification and acetyl (Protein N-term), pyrolysine from E, pyrolysine from Q and oxidation (M) as variable modifications. Peptide mass tolerance was set to ± 25 ppm for precursors and 0.05 Da for fragment masses. The confidence interval for protein identification was set to $\geq 95\%$ ($P < 0.05$), and only peptides with an individual ion score above the 1% false discovery rate (FDR) at spectra level were considered correctly identified.

Protein-protein interaction (PPI) networks were analyzed using STRING v10.5 (<http://string.embl.de/>) (26), with a medium confidence threshold score of 0.4. The *Homo sapiens* model organism was used for the analysis. Gene symbols were obtained through sequence homology with *H. sapiens* orthologs using Blast2GO version 4.1.9.

Shotgun Proteomics for IFIT5 Peptide Validation

Nano LC ESI-MS/MS analysis was performed using an Eksigent 1D-nanoHPLC coupled to a 5600 TripleTOF QTOF mass spectrometer (SCIEX). The analytical column was a silica-based, reversed-phase nanoACQUITY UPLC 75 $\mu\text{m} \times 15\text{ cm}$, 1.7 μm particle size (Waters Corporation, Milford, MA, USA). The trap column was an Acclaim PepMap 100, 5 μm particle diameter, 100 Å pore size, switched online with the analytical column. The loading pump delivered a solution of 0.1% formic acid in 98% water/2% acetonitrile (Scharlab, Barcelona, Spain) at 3 $\mu\text{L}/\text{min}$. The nanopump provided a flow rate of 250 nL/min and was operated under gradient elution conditions using 0.1% formic acid (Fluka, Buchs, Switzerland) in water as mobile phase A and 0.1% formic acid in 100% acetonitrile as mobile phase B. Gradient elution was performed according to the following scheme: isocratic conditions of 96% A:4% B for 5 min, linear increase to 40% B at 25 min, linear increase to 95% B after 2 min, isocratic conditions of 95% B for 5 min, and return to initial conditions after 10 min. Injection volume was 5 μL . The LC system was coupled via a nanospray source to the mass spectrometer. Automatic data-dependent acquisition using dynamic exclusion allowed both full scans of (m/z 350–1,250) MS spectra and tandem MS CID spectra of the 15 most abundant ions. Acquisition time was 250 and 100 ms for MS and MS/MS spectra, respectively. The candidate peptide was synthesized using standard Fmoc chemistry in an Intavis Multiple peptide synthesizer (INTAVIS, Cologne, Germany). The synthetic peptide was used to confirm the peptide sequence identified by shotgun proteomics.

Time Course of *ifit5* Expression in Rainbow Trout RBCs and RTG-2 Exposed to VHSV

Ficoll-purified RBCs (10^6 cells/well) and RTG-2 cells (2.5×10^5 cells/well) were exposed to VHSV at MOI 1 at different time points (0, 3, 6, 24, and 72 h). Cells were resuspended and stored

in appropriate buffer for RNA extraction. The expression levels of NVHSV and the *ifit5* gene were analyzed by real time RT-qPCR.

Rainbow Trout Anti-IFIT5 Antibody Production

Rainbow trout anti-IFIT5 antibody was designed and produced at Dr. Luis Mercado's laboratory. First, antigenic propensity from different regions of the rainbow trout IFIT5 protein sequence (GenBank: AAM18469.1) were identified, analyzing hydrophobicity (Hopp & Woods test), accessibility, and flexibility. Then, peptides from the most antigenic regions were selected for peptide synthesis. Before synthesis, peptide sequences were modified by replacing cysteine residues with serine residues to avoid formation of intrachain disulfide bonds. Cysteine was added to the start and end of the peptide sequence to produce dimers. Peptide synthesis was performed using mesh packets with resin as previously described (27). Peptide cleavage was performed using cold petroleum ether. After cleavage of the peptide from the resin, peptides were characterized by MALDI-TOF (Bruker Daltonics Inc, Billerica, MA). Oxidation of peptides was performed by dilution of the peptide in milliQ water and agitating overnight. After oxidation, peptides were purified using G10 resin (Sigma-Aldrich) to eliminate salts.

To immunize mice against the peptides, 100 μg of oxidized peptide was conjugated with Freund's adjuvant (Thermo Fisher Scientific) following the manufacturer's instructions. The mix was subcutaneously injected into mice. A total of 3 injections were made with a lapse of 2 weeks between them. After all immunizations were done, euthanasia was carried out with anesthetic overdose. Blood was collected by cardiac injection. Blood sera were obtained by letting blood coagulate for 30 min at 37°C followed by an incubation at 4°C for 1 h. Finally, blood was centrifuged at 5,000 rpm for 10 min, and serum was collected. An ELISA was performed to determine the serum titers (Supplementary Figure 1). Wells were coated with 100 ng of the corresponding peptides diluted in 100 μL of PBS overnight at 4°C. Blank wells were coated using only PBS. Then, PBS with peptides was removed and wells were washed 3 times with PBS. Then, 5% non-fat milk was used to block the wells at 37°C in agitation for 2 h. Sera were diluted in PBS (from 1/500 to 1/64,000) and incubated at 37°C for 90 min. Wells were further washed 3 times and incubated with goat anti-mouse HRP-conjugated antibody diluted 1/7,000 for 1 h at 37°C in agitation. Each well was incubated with 100 μL of 3,3',5,5'-tetramethylbenzidine (Thermo Fisher Scientific) for 15 min. The reaction was stopped with 50 μL 1 N sulfuric acid (Winkler Ltda, Santiago, Chile). Plates were read at 450 nm using VersaMax™ Tunable microplate reader (Molecular Devices LLC, San Jose, CA, USA). Anti-IFIT5 antibody was validated by western blot (Supplementary Figure 1). RBC cell pellets were homogenized and applied into Tris-Glycine sodium dodecyl sulfate 12% polyacrylamide gels under reducing conditions as previously described (4). Briefly, proteins in the gel were transferred to a nitrocellulose membrane (BioRad, Madrid, Spain) and blocked with 8% dry milk and 1% Tween-20 in PBS. Then, the membrane was incubated with the antibody diluted 1/500 in PBS containing 0.5% dry milk and 0.5% Tween-20 (PMT buffer), overnight

at 4°C. Finally, the membrane was washed and incubated with secondary antibody goat anti-mouse peroxidase (Sigma-Aldrich) in PMT buffer for 45 min, and proteins were detected with ECL chemiluminescence reagents (Amersham Biosciences, Buckinghamshire, UK) and revealed by exposure to an X-ray film.

Flow Cytometry and Immunofluorescence of IFIT5

RBCs were fixed, permeabilized, and incubated with primary and secondary antibodies as previously described (4). Mouse anti-IFIT5 antibody at 1/300 dilution in permeabilization buffer and rabbit anti-GVHSV antibody (kindly provided by Dr. Neils Lorenzen to Dr. Julio Coll) at 1/300 dilution in permeabilization buffer were used as primary antibodies. Secondary antibodies used in these studies included anti-mouse IgG CFTM 488 and anti-rabbit IgG CFTM 647 (Sigma-Aldrich) produced in goat. Flow cytometry analysis was performed using a FACSCanto II (BD Biosciences, Madrid, Spain) flow cytometer. A total of 30,000 events were acquired. Gating selection for RBCs is shown in **Supplementary Figure 2**. To obtain immunofluorescence images, cells were incubated with 4',6-diamidino-2'-phenylindole dihydrochloride (DAPI) (Sigma-Aldrich) at 0.3 pg/mL for 5 min to stain the cell nucleus. Immunofluorescence images were taken with the IN Cell Analyzer 6000 (GE Healthcare).

Molecular Docking Procedure to Search for IFIT5 Modulators

The crystal structure of the IFIT5 protein has been solved in human (28), but not rainbow trout. Therefore, we constructed a model using rainbow trout IFIT5 amino acid sequences (GenBank AAM18469.1) and human IFIT5 protein as template. A homology modeling approach for rainbow trout IFIT5 was performed using the Swiss-Model server (29) and the crystal structure of human IFIT5 (PDB number 5UDL).

The crystal structure of IFIT5 showed an RNA-binding pocket cavity (28). Therefore, we searched for compounds capable of binding to this cavity to modulate its functions. The screen resulted in a list of 325,508 natural compounds from the SuperNatural II database (19). Mol2 files were converted into pdbqt format using the Python script "prepare_ligand4.py" included in the AutoDockTools-1.5.7.rc1 (30, 31).

Prior to the docking procedure, the protein (receptor) and ligand structures were prepared as previously described (30, 31). The IFIT5 modeled protein structure was subjected to geometry optimization using the repair function of the FoldX algorithm (32). The docking procedure was performed with AutoDock/Vina (33) as described (31, 34). Compounds with the lowest calculated Gibbs free energy variations ($\Delta G \leq -11$ kcal/mol) were selected as putative modulators.

In silico Analysis of Pharmacokinetic Parameters and Toxicity Potential Properties of the Modulator Candidates

DataWarrior v4.2.2 software (Allschwil, Switzerland) (35) was used to calculate molecular descriptors, such as the topological

polar surface area (TPSA), molecular weight (MW), estimated logarithm (base 10) of the solubility measured in mol/L (logS), estimated logarithm (base 10) of the partition coefficient between n-octanol and water (logP), number of hydrogen bond acceptors, number of hydrogen bond donors, violations of Lipinski's rule of 5 (36), drug score, and fragment-based druglikeness. The *in silico* absorption, distribution, metabolism, excretion, and toxicity (ADMET) properties of all compounds were calculated using admetSAR (37) and DataWarrior v.4.2.2 software. The selected compounds were purchased from the chemical supplier MolPort (MolPort SIA, Riga, Latvia).

Modulating IFIT5 Activity With Selected Compounds

The compounds were resuspended in dimethyl sulfoxide (DMSO) (Sigma-Aldrich) at a concentration of 10 mM and diluted in RPMI 10% FBS to concentrations ranging from 540 to 4,860 nM. To evaluate the toxicity of the compounds in RBCs, the LIVE/DEAD[®] Cell Vitality Assay Kit (Thermo Fisher Scientific) was used according to the manufacturer's instructions. Briefly, RBCs were incubated with different concentrations of the compounds in RPMI 10% FBS for 24 h at 14°C. Then, LIVE/DEAD imaging reagents were mixed at equal volumes and added to the cells and incubated for 15 min at room temperature. Samples were analyzed using the FACSCanto II (BD Biosciences) flow cytometer. Live cells fluoresce green (calcein AM substrate), and dead cells fluoresce red (ethidium homodimer-1 [EthD-1]). Each subpopulation was separated into 4 quadrants. The percentage of cell viability was calculated as follows: [number of green-stained cells in treated RBCs/number of green-stained cells in non-treated RBCs] x 100. A total of 20,000 events were acquired. RBCs treated with 100 μ M of H₂O₂ (Sigma-Aldrich) were used as a positive control for dead RBCs.

To evaluate IFIT5 activity modulation by the compounds, RBCs were incubated with 4,860 nM of the compounds for 24 h. After removing the compounds, cells were washed with culture medium and then exposed to VHSV at MOI 1 for 24 h at 14°C. Samples were stored in buffer for RNA extraction, and RT-qPCR was performed.

Modulating IFIT5 RNA-binding Pocket Cavity With VHSV RNA

RNA was isolated from VHSV (4*10⁸ PFU/mL) as described below. Then, RBCs were electroporated with 5 μ L VHSV RNA using the NeonTM Transfection System (Life Technologies, Thermo Fisher Scientific), at 1,600 V, 30 ms, and 1 pulse. After 24 h of incubation, RBCs were washed with culture medium and exposed to VHSV MOI 1. After 3 h of incubation at 14°C, samples were washed with culture medium and some samples were stored in buffer for RNA extraction while others were further incubated for 24 h. The cell pellets of these samples were stored in RNA extraction buffer.

IFIT5 Small Interfering RNA (siIFIT5) Assay

Three different IFIT5 small interfering RNA sequences (siIFIT5) were designed and produced by Sigma-Aldrich (**Table 1**). RBCs were transfected with a mixture of 3 siIFIT5 sequences by

TABLE 1 | Sequences of rainbow trout *ifit5*-specific siRNA.

Name	siRNA design sequence (5'-3')	Start on target
siIFIT5-1 sense	GGUAAUCCAAGGGCCUCAAdTdT	432
siIFIT5-1 antisense	UUGAGGCCCUUGGAUACcTdT	432
siIFIT5-2 sense	CAAUGAGUCCCUACACAUUdTdT	857
siIFIT5-2 antisense	AAUGUGUAGGGACUCAUUGdTdT	857
siIFIT5-3 sense	CAGCUUACCUUCAGUACAUdTdT	461
siIFIT5-3 antisense	AUGUACUGAAGGUAAGCUGdTdT	461

electroporation. For each electroporation reaction, we used 187 pmol of each siRNA per 0.5×10^6 cells resuspended in Buffer T (Neon™ Transfection System Kit, Life Technologies). As a negative control, 187 pmol siGFP was used (Sigma-Aldrich). RBCs were electroporated as described above and incubated for 3 days at 14°C.

IFT5 silencing was evaluated at transcript and protein level. *ifit5* gene silencing was analyzed by RT-PCR, described in section RNA Isolation and Gene Expression by RT-PCR and RT-qPCR. Moreover, IFIT5 silencing was determined by western blot, described in section Rainbow Trout Anti-IFIT5 Antibody Production, using anti-IFIT5 antibody at 1/500 dilution and anti- α -actin antibody (Sigma-Aldrich) (1/100) was used as endogenous control. Goat anti-mouse peroxidase and goat anti-rabbit peroxidase (Sigma-Aldrich), were respectively used for anti-IFIT5 and anti- α -actin antibodies.

Transfected RBCs were separately exposed to VHSV MOI 1 at 14°C. After 3 h of VHSV exposure, RBCs were washed with culture medium and incubated for 24 h. Cells were resuspended and stored in appropriate buffer for RNA extraction.

RNA Isolation and Gene Expression by RT-PCR and RT-qPCR

RNA was isolated using the E.Z.N.A.® Total RNA Kit (Omega Bio-Tek Inc., Norcross, GA). Subsequent DNase treatment was done using TURBO™ DNase (Ambion, Thermo Fisher Scientific) as previously described (4). Then, cDNA synthesis from RNA samples were performed as described in Chico et al. (38) using M-MLV reverse transcriptase (Invitrogen, Thermo Fisher Scientific).

To evaluate *ifit5* gene silencing, cDNA from siRNA-treated samples were analyzed by semiquantitative RT-PCR. PCR amplification reactions were performed as follows: 0.5 μ L dNTP mix (10 mM each) (Invitrogen, Thermo Fisher Scientific), 0.125 μ L GoTaq® DNA polymerase (Promega Biotech, Madrid, Spain), 5 μ L 5X Green GoTaq® reaction buffer (Promega Biotech), 0.5 μ L each primer (20 μ M) (Table 2), and 2.5 μ L cDNA in a total volume of 25 μ L. PCRs were carried out in a GeneAmp® PCR System 2700 thermocycler (Applied Biosystems, Thermo Fisher Scientific). Cycling conditions were 94°C for 5 min followed by 30 cycles at 94°C for 1 min, specific annealing temperature (Table 2) for 1 min and 72°C for 90 s. Then, 1 cycle at 72°C was held for 7 min. Glyceraldehyde 3-phosphate dehydrogenase (GAPDH) (39) (Table 2) was used as

a housekeeping gene to normalize the RT-PCR. PCR products were visualized on a 1.2% agarose gel stained with Gelred® nucleic acid stain (Biotium, Inc. Fremont CA, USA). NVHSV and *ifit5* genes were analyzed by real-time RT-qPCR. RT-qPCR was carried out using the ABI PRISM 7300 System (Thermo Fisher Scientific). Cycling conditions and gene expression analysis methods have been previously described (4). Primers and probes are listed in Table 3. The *efl α* and eukaryotic 18S rRNA genes (Cat#4310893E, Thermo Fisher Scientific) were used as endogenous controls.

In situ Proximity Ligation Assay (PLA)

Ficoll-purified RBCs from rainbow trout blood were exposed to VHSV MOI 1 for 6 h at 14°C. Unexposed and VHSV-exposed RBCs were attached to frosted slides (Thermo Fisher). The attached cells were fixed with 4% paraformaldehyde (PFA) for 1 h at room temperature. Then, samples were washed 3 times with PBS. The slides were incubated with 70% ethanol for 30 s, placed on ice for 60 min, and air-dried. Finally, slides were stored at -20°C until PLA. PLA recognizes close-proximity proteins (40 nm) by primary antibodies, which are then recognized by secondary antibodies conjugated to specific oligonucleotides. Subsequently, a ligase and complementary oligonucleotides are added and a circle is formed, which is amplified by rolling circle amplification. The amplification product is detected with fluorescent oligonucleotides (42). The PLA was performed using Duolink® *in situ*-Fluorescence kit (Sigma-Aldrich) following the manufacturer's instructions. Briefly, blocking solution was added to each sample, and the slides were incubated in a humidity chamber for 1 h at 37°C. After that, the blocking solution was tapped off and slides were incubated with a primary antibody against IFIT5 protein produced in mice and against GVHSV protein produced in rabbit diluted at 1/300 in a volume of 100 μ L overnight at 4°C in a humidity chamber. Detection was performed using PLA secondary probes and ligation according to the manufacturer's instructions. Finally, the slides were mounted with a cover slip using Duolink *in situ* Mounting Medium with DAPI and stored at -20°C until analysis. All imaging pictures were taken with the IN Cell Analyzer 6000 (GE Healthcare). Positive cells were counted using a designed routine in the IN Cell Analyzer workstation 3.7.2 software.

Software and Statistics

Graphpad Prism 6 software (www.graphpad.com) was used for statistics calculations and graphic representation. Statistic tests and associated *P*-values are indicated in each assay. Flow cytometry data were processed and analyzed using Flowing Software 2.5.1 (www.flowingsoftware.com/).

RESULTS

Immunoprecipitated Proteins From VHSV-exposed RBCs

It was recently reported that VHSV infection appeared to be halted in rainbow trout RBCs (4). However, specific RBC proteins that interact directly with VHSV have not been identified. To address this question, lysates of VHSV-exposed

TABLE 2 | Sequences of primers and probes for RT-PCR.

Gene	Forward primer (5' - 3')	Reverse primer (5' - 3')	Annealing T ^a (C°)	Reference or accession number
<i>ifit5</i>	TCTACAGGGGGAGCCAAACA	AGGGCTAGGAGGACCATGAC	60	AF483530.1
<i>gapdh</i>	ATGTCAGACCTCTGTGTTGG	TCCTCGATGCCGAAGTTGTCG	52	(39)

TABLE 3 | Sequences of primers used for RT-qPCR.

Gene	Forward primer (5' - 3')	Reverse primer (5' - 3')	Probe (5'-3')	Reference or accession number
<i>ifit5</i>	CCCTCAATGACTCTGACAAGCA	CCCTGCCCTCATCTTCTTCT	CCAGCTTCGGCCTGTTTCTGTTCCA	(40)
NVHSV	GACTCAACGGGACAGGAATGA	GGGCAATGCCCAAGTTGTT	TGGGTTGTTCAACCAGGCCGC	(38)
<i>ef1α</i>	ACCCTCCTCTTGGTCGTTTC	TGATGACACCAACAGCAACA	GCTGTGCGTGACATGAGGCA	(41)

RBCs were immunoprecipitated with monoclonal antibody against N protein of VHSV because NVHSV is one of the major structural components of VHSV (43) and therefore is an ideal candidate to identify potential protein interactions. The resulting immune complexes were analyzed by mass spectrometry. A total of 31 proteins were identified in the immunoprecipitate (IP) of VHSV-exposed RBCs (Table 4; Supplementary Table 1). Importantly, the NVHSV protein was identified among the IP proteins (Supplementary Table 1). An interactome network was built for these proteins to reveal protein-protein interactions and predict functional associations using STRING software. As shown in Figure 1, 23 proteins highly interacted with each other, with a PPI enrichment $P < 0.05$, and 9 proteins did not show interaction. Predicted functional associations of these proteins were related to: (i) translation elongation (eukaryotic translation elongation factor 1 alpha [EEF1A1], ribosomal protein S4 X-linked [RPS4X], ribosomal protein L5 [RPL5], ribosomal protein L7 [RPL7], ribosomal protein L15 [RPL15], ribosomal protein S16 [RPS16], and ribosomal protein S26 [RPS26]); (ii) viral transcription (RPS4X, RPL5, RPL7, RPL15, RPS16, and RPS26); (iii) viral process (RPS4X, RPL5, RPL7, RPL15, RPS16, RPS26, apolipoprotein E [APOE], heat shock 70 kDa protein 8 [HSPA8], and proteasome [prosome, macropain] subunit alpha type 7 [PSMA7]); and (iv) immune system process (alpha-2-glycoprotein 1, zinc-binding [AZGP1], apolipoprotein B [including Ag(x) antigen, APOB], peroxiredoxin 1 [PRDX1], PSMA7, S100 calcium binding protein A9 [S100A9], glyceraldehyde-3-phosphate dehydrogenase [GAPDH], actin beta [ACTB], actin gamma 1 [ACTG1], bleomycin hydrolase [BLMH], and interferon-induced protein with tetratricopeptide repeats 5 [IFIT5]).

Among all identified proteins, we focused on IFIT5 because the IFIT family has recently emerged as an important player in antiviral innate immunity (12–18). To validate IFIT5 in the IP sample, a synthetic peptide was synthesized and a Nano LC ESI-MSMS analysis was performed. The synthetic peptide resulted in the same mass spectrum fragmentation obtained from IP peptide. Therefore, the synthetic peptide confirmed IFIT5 found by shotgun proteomics (Supplementary Figure 3).

IFIT5 Gene and Protein Expression in Rainbow Trout RBCs After VHSV Exposure

A time course assay was performed to determine gene and protein expression of rainbow trout IFIT5 in VHSV-exposed RBCs. Ficoll-purified RBCs were exposed to VHSV at MOI 1, and the expression levels of IFIT5 transcript and protein were evaluated at different time points by RT-qPCR and flow cytometry, respectively. VHSV replication in RBCs was evaluated at each time point by RT-qPCR using the N gene of VHSV. The *ifit5* gene transcripts started to increase by 3 hpe in RBCs, which correlated with the time point of the highest VHSV replication (Figure 2A). By 6 hpe, VHSV replication began to decrease, which coincided with the highest transcriptional and protein expression level of IFIT5, Figures 2A–D). After this time, IFIT5 transcripts and protein levels decreased (Figures 2A,B), and *ifit5* transcripts reached the basal level at 72 hpe (Figure 2A). Colocalization between IFIT5 and GVHSV was observed by immunofluorescence imaging (Figure 2D). A similar time course assay was performed in RTG-2 cells, another fish cell line (Supplementary Figure 4). *ifit5* gene expression in RTG-2 increased in VHSV-infected cells at 24 hpe, but this *ifit5* upregulation was not enough to decrease VHSV replication. At 72 hpe, the cell monolayer was destroyed.

PLA Between IFIT5 and GVHSV

To investigate possible interactions or proximity (proteins within 40 nm) between IFIT5 and VHSV, and to further corroborate the colocalization between IFIT5 and GVHSV observed by immunofluorescence (Figure 2D), a PLA was performed. We selected the GVHSV protein because it is the major surface protein of the virion. The highest IFIT5 expression level was observed at 6 hpe to VHSV, so we chose this time point to perform the PLA. Cells with red dots inside the cytoplasm were considered positive (Figure 3A). VHSV-exposed RBCs had significantly more positive cells than control RBCs (Figure 3B).

TABLE 4 | Mass spectrometry proteomic analysis of immunoprecipitated proteins from VHSV-exposed RBCs.

Main accession	<i>Homo sapiens</i> ortholog gene symbol	Gene description	Mascot score	N° of peptide sequences identified
A0A0B5E7Z4	ACTB	Actin beta	675	9
A0A146YS88	ACTG1	Actin gamma 1	63	1
W5N1H4	ANXA6	Annexin A6	53	1
P04114	APOB	Apolipoprotein B (including Ag(x) antigen	112	2
H0Y7L5	APOE	Apolipoprotein E	56	1
P25311	AZGP1	Alpha-2-glycoprotein 1, zinc-binding	87	1
J3KSD8	BLMH	Bleomycin hydrolase	55	1
H2TZ44	DZIP1	DAZ interacting protein 1	49	1
Q2TS51	EEF1A1	Eukaryotic translation elongation factor 1 alpha	170	3
C1J0I5	ENO1	Enolase 1	114	2
K7EPH2	FARSA	Phenylalanyl-tRNA synthetase, alpha subunit	54	1
C1BLG8	GAPDH	Glyceraldehyde-3-phosphate dehydrogenase	58	1
X1WG17	HIST2H2BE	Histone cluster 2, H2be	253	4
Q5GAW2	HIST2H3D	Histone cluster 2, H3d	58	1
A0A0C5BIF3	HSPA8	Heat shock 70kDa protein 8	140	2
A0A068FNU8	IFIT5	Interferon-induced protein with tetratricopeptide repeats 5	51	1
I6WP32	MYH6	Myosin, heavy chain 6	53	1
A0A1A7WCM1	PIBF1	Progesterone immunomodulatory binding factor 1	51	1
A0A060YDT1	PRDX1	Peroxiredoxin 1	64	1
A0A060XGK1	PSMA7	Proteasome (prosome, macropain) subunit, alpha type, 7	51	1
Q1JQ20	RIC8B	Resistance to inhibitors of cholinesterase 8 homolog B	53	1
A0A0S7EQ42	RPL15	Ribosomal protein L15	71	1
A0A060WXW6	RPL5	Ribosomal protein L5	59	1
A0A143WEA0	RPL7	Ribosomal protein L7	48	1
A0A0E9WET2	RPS16	Ribosomal protein S16	137	2
A0A0P7TLE4	RPS26	Ribosomal protein S26	57	1
A0A087XME4	RPS4X	Ribosomal protein S4, X-linked	51	1
P06702	S100A9	S100 calcium binding protein A9	75	1
A0A060W847	SLK	STE20-like kinase	51	1
M4A1M1	TKT	Transketolase	50	1
A0A060WX95	TUBA1B	Tubulin, alpha 1b	77	1

Analysis of Compounds Docked to RNA-binding Pocket Cavity of IFIT5

One of the established antiviral mechanisms of the IFIT family is recognition of viral mRNA (14–16) by the RNA-binding pocket cavity (28). Therefore, we searched for natural compounds that could bind to the IFIT5 RNA-binding pocket cavity and modulate its function. Natural compounds from the SuperNatural II database (19) were screened with a docking procedure. Starting from a library of 325,508 compounds, molecular docking experiments resulted in selection of compounds with a low Gibbs free energy variation value (ΔG , kcal/mol), and then of potentially higher affinity. We used the 3D model of rainbow trout IFIT5 (29) to carry out the molecular docking experiments at the RNA-binding pocket cavity. Up to 20 poses per compound bound to the explored RNA-binding site cavity (Figure 4A) were achieved. Overall, 0.16% ($n = 507$) of compounds had a $\Delta G \leq -11.5$ kcal/mol. Additional filters were applied until a reasonable number of candidate compounds were obtained.

We analyzed 13 ADMET parameters for each compound, and only compounds with values within the limits of each parameter as described by Ruiz-Torres et al. (31) passed through this screen. After ensuring commercial availability, 19 compounds were selected as candidates for IFIT5 modulators (Supplementary Table 2). The molecular structures of these compounds were compared, resulting in different clusters with up to 70% identity. This strategy allowed us to choose at least one representative compound of each cluster to experimentally test for IFIT5 modulating activity. Ultimately, 3 compounds (SN00105976, SN00110204, and SN00130855) were selected for experimental testing.

Modulating IFIT5 Protein in RBCs

The percentage of viability in RBCs treated with the 3 selected potential IFIT5 modulator compounds (concentrations ranging from 540 nM to 4,860 nM) was >99.9% for compounds SN00105976 and SN00130855. We used these 2 compounds in additional assays to test their ability to modulate IFIT5 function.

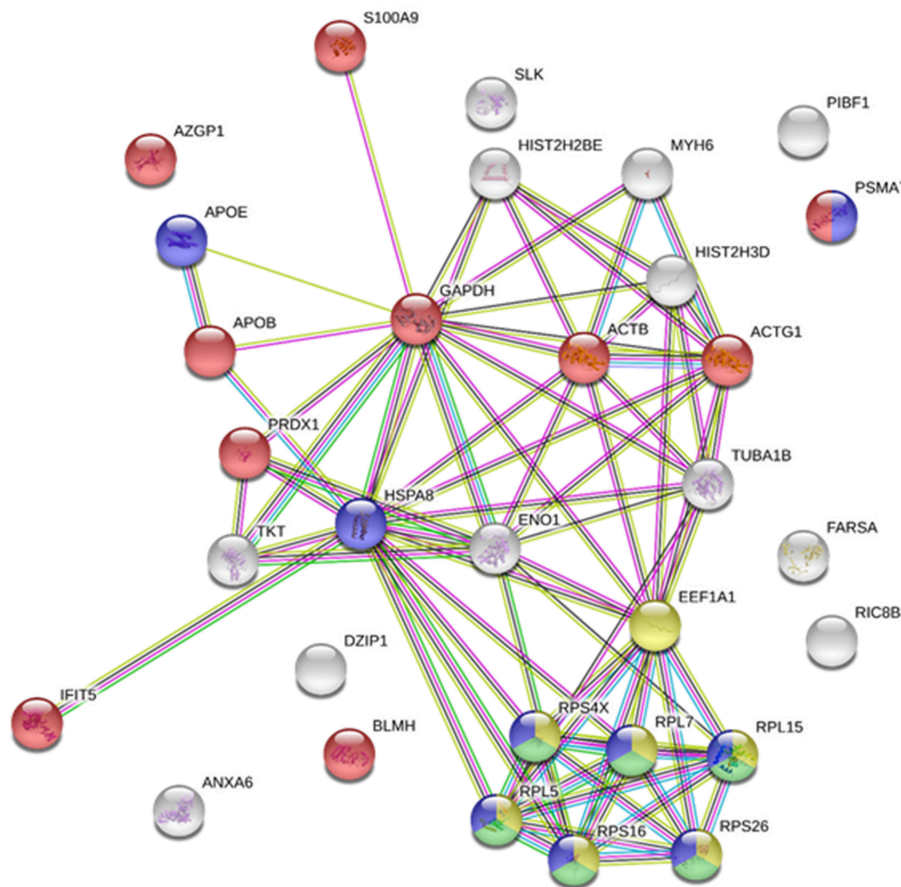


FIGURE 1 | Immunoprecipitated proteins from RBCs exposed to VHSV. Lysates from RBCs exposed to VHSV at MOI 1 for 3 h were immunoprecipitated (IP) with monoclonal antibody against N protein of VHSV (2C9). The IP complex was precipitated with protein A Sepharose 4 Fast Flow beads. The obtained proteins were analyzed by mass spectrometry. A representation of constructed protein-protein interactions of IP proteins is shown. Nodes represent proteins, and edges denote the interactions between 2 proteins. Node colors indicate proteins functionally annotated with STRING software. Red, immune system process; blue, viral process; yellow, translation elongation; green, viral transcription.

We evaluated the modulatory activity of the compounds on IFIT5 antiviral function in RBCs by exposing compound-treated RBCs to VHSV and evaluating VHSV replication. **Only SN00105976 appeared to modulate IFIT5 antiviral function: RBCs incubated with this compound at 4,860 nM for 24 h showed a significant increase in VHSV replication (Figure 4B).**

We also performed an indirect assay to modulate the IFIT5 RNA-binding pocket cavity by pretreating RBCs with VHSV RNA (presumably the IFIT5 target). We assumed that preincubating RBCs with VHSV RNA would result in competition with viral RNA for the IFIT5 binding pocket cavity and hence increase viral replication. As expected, **RBCs electroporated with VHSV RNA showed an increase in VHSV replication (Figure 4C).**

Silencing *ifit5* Gene Expression

To further evaluate the role of IFIT5 in the antiviral mechanisms of rainbow trout RBCs, we performed *ifit5* gene silencing assays using siRNA. After silencing *ifit5*, its expression in RBCs decreased in RT-PCR experiments (**Figure 5A**) and in western

blot assay (**Figure 5B**). We noted a significant increase in VHSV replication in RBCs pretreated with siIFIT5 sequences in RT-qPCR experiments (**Figure 5C**).

DISCUSSION

A wide variety of defense mechanisms have been reported for nucleated RBCs in response to VHSV exposure (4). To identify which rainbow trout RBC proteins interact directly with VHSV, we characterized the immunoprecipitated proteome of VHSV-exposed RBCs using an antibody against the N protein, which constitutes one of the major structural components of VHSV (43). The IP proteomic characterization included 31 proteins by mass spectrometry analysis. It should be taken into account that many of the proteins detected in the IP could have been immunoprecipitated due to a nucleation effect of protein-protein interactions in the protein milieu. However, an interactome network from the IP proteins revealed interesting functional associations, such as translation elongation, viral

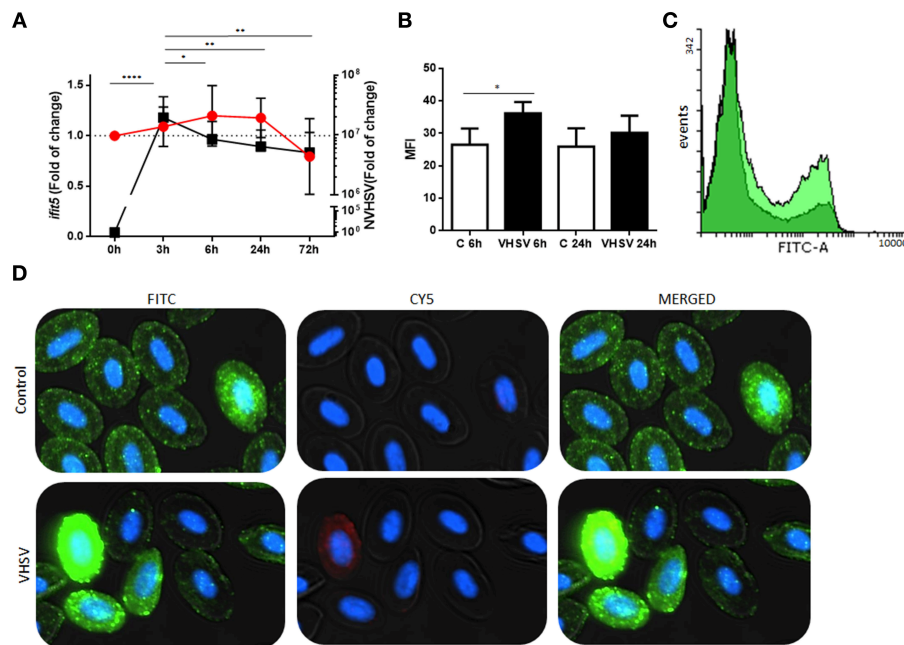


FIGURE 2 | Time course of NVHSV gene replication and *ifit5* gene expression in VHSV-exposed rainbow trout RBCs. **(A)** Ficoll-purified RBCs were exposed to VHSV MOI 1 for different amounts of time (0, 3, 6, 24, and 72 hpe). The N gene of VHSV (NVHSV, black square) and *ifit5* (red circle) gene expression profiles were analyzed by RT-qPCR. Gene expression was normalized to the reference gene *ef1α* and relativized to control cells (RBCs unexposed to VHSV). Data represent the mean \pm SD, $n = 7$. Tukey's multiple comparison test was performed for statistical analysis among all time points. *, **, and **** indicate $P < 0.05$, < 0.01 , and < 0.0001 , respectively, for NVHSV. Lines indicate the trend followed by VHSV (black) and *ifit5* (red) during the time course assay. **(B)** IFIT5 protein expression observed in RBCs exposed to VHSV MOI 1 at 6 and 24 hpe were evaluated via flow cytometry using mouse anti-IFIT5 primary antibody and anti-mouse IgG CFTM 488 as a secondary antibody. Mean fluorescent intensity (MFI) is shown. Data represent the mean \pm SD, $n = 4$. Kruskal-Wallis Test with Dunn's multiple comparison *post-hoc* test was performed in comparison with control ($*P < 0.05$). **(C)** Representative flow cytometry overlay histograms showing unexposed RBCs (dark green) and VHSV-exposed RBCs at MOI 1 after 6 hpe (bright green). **(D)** Representative costaining immunofluorescence of IFIT5 and GVHSV in RBCs unexposed (control) or exposed to VHSV MOI 100, at 6 hpe, using antibodies against IFIT5 and GVHSV proteins. IFIT5 is stained green (anti-mouse IgG CFTM 488 secondary antibody), GVHSV is stained red (anti-rabbit IgG CFTM 647 secondary antibody), and nuclei are stained with DAPI. The image was taken at 60X magnification.

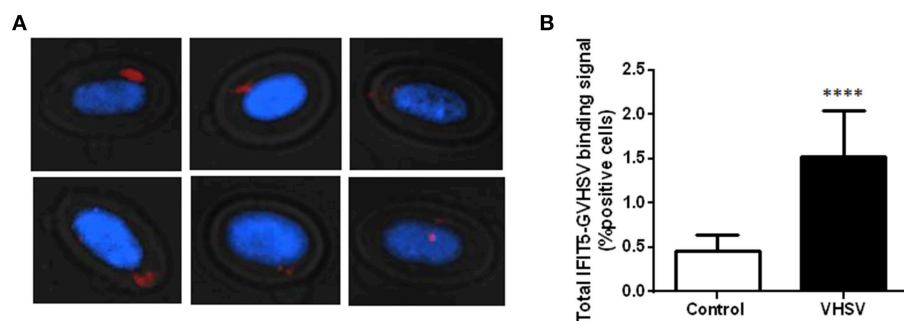


FIGURE 3 | Imaging and quantification of PLA between IFIT5 and GVHSV. RBCs exposed to VHSV MOI 1 for 6 h were subjected to a PLA using specific antibodies against IFIT5 and protein G of VHSV. **(A)** Representative images of cells showing IFIT5-GVHSV colocalization (cells with red dots inside). Fluorescence images were taken at 60X magnification. Nuclei were stained with DAPI. **(B)** Graph representing the percentage of IFIT5-GVHSV-positive cells in the PLA. Data represent the mean \pm SD, $n = 3$. A Mann-Whitney test was performed for statistical analysis. **** $P < 0.0001$.

transcription, viral process, and immune system process. Similar cellular proteins have been found in dengue virus (DENV)-infected human hepatic cells (Huh-7) in a combined immunoprecipitation assay using anti-NS1 antibody from DENV and affinity chromatography assay (45). Among them, they

identified GAPDH, EEF1A1, histones, heat shock proteins, PRDX, tubulin, and ribosomal proteins. Ribosomal proteins were the most abundant proteins identified (50%) (45). In our study, 20% of identified proteins were ribosomal proteins. The main function of the ribosomal proteins is mRNA translation.

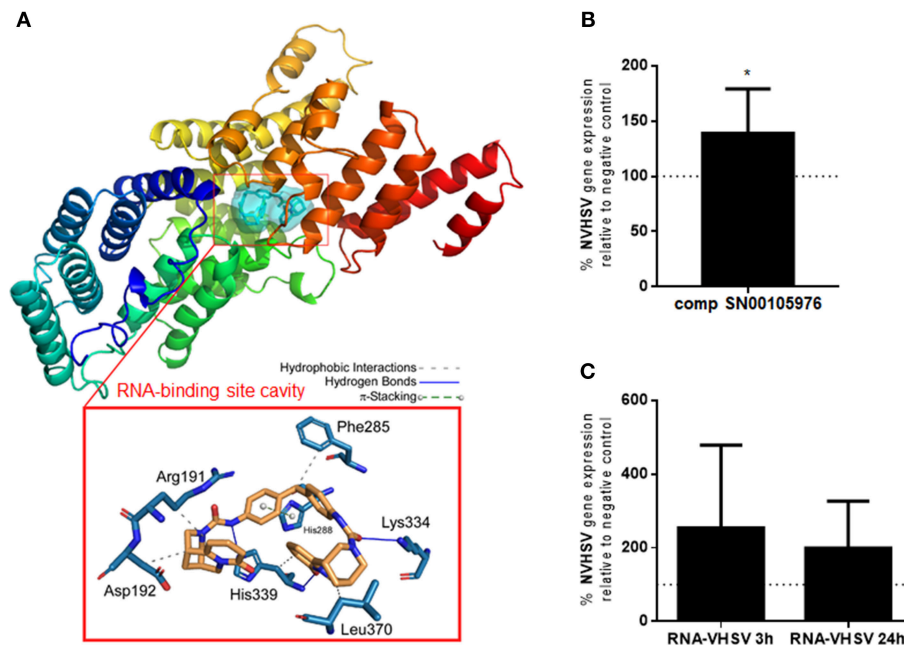


FIGURE 4 | IFIT5 modulation increases VHSV replication. (A) Molecular docking analysis for the selected compound SN00105976 against IFIT5 RNA-binding pocket cavity. The secondary structure of the IFIT5 protein is shown from the N terminus (blue) to the C-terminus (red), and pictures the compound interacting in the IFIT5 RNA-binding pocket cavity. The compound and IFIT5 RNA-binding pocket-interacting residues of the binding site and each type of molecular interaction are expanded in the bottom red box. Interactions were detected with the Protein–Ligand Interaction Profiler (PLIP) algorithm (44). (B) RBCs incubated with 4,860 nM of compound SN00105976 for 24 h and exposed to VHSV MOI 1 for 24 h. The percentage of VHSV replication relative to VHSV-exposed RBCs (negative control) was determined by RT-qPCR of the NVHSV gene. Data represent the mean \pm SD, $n = 7$. A Wilcoxon matched-pairs signed rank test was performed for statistical analysis. * $P < 0.05$. (C) RBCs electroporated with VHSV RNA and incubated for 24 h before being exposed to VHSV MOI 1 for 3 or 24 h. Gene expression was normalized to the eukaryotic 18S rRNA gene. Percentage of VHSV replication relative to VHSV-exposed RBCs (negative control) was determined by RT-qPCR of the NVHSV gene. Data represent the mean \pm SD, $n = 3$. A Wilcoxon matched-pairs signed rank test was performed for statistical analysis.

However, several ribosomal proteins have other functions, such as regulatory functions in fundamental processes related to the cell cycle, apoptosis, development, and oncogenes (46–48). It is well-known that **viruses depend on ribosomes to synthesize proteins** (49). Several ribosomal genes or proteins have a significant association with virus. For example, the ribosomal protein RPL18 interacts with the DENV NS1 protein and is required during its replicative cycle (45). RPL18 and RPL7 have been also found in siRNA screens performed with yellow fever and West Nile virus (50). In addition, RPL6, RPL3, and RPL15 were significantly associated with viral acute respiratory infection in infants (49). Moreover, RPS4X mRNA interacts with nonstructural protein 5B (NS5B) of hepatitis C virus (51). Also, vesicular stomatitis virus (VSV) mRNA translation depends specifically on the 60S ribosomal protein RPL40 (52). We also found glyceraldehyde 3-phosphate dehydrogenase, GAPDH, an important metabolic enzyme, which has been described to interact with some viruses such as Japanese encephalitis virus (53), human immunodeficiency virus type 1 (54, 55), cucumber mosaic virus (56), DENV (57), bamboo mosaic virus (58), hepatitis A virus (59), and human parainfluenza virus type 3 (60). Therefore, GAPDH is important in some viral infections, but we do not know how GAPDH interacts with VHSV nor the biological significance of this interaction.

Several proteins related to the immune system were identified in the IP proteomic characterization. We identified the S100A9 protein, which has been recently classified as a novel damage-associated molecular pattern, and has been associated with hepatitis B virus infection (61) and bovine viral diarrhea virus (BVDV), which interacts with BVDV Npro protein to decrease virus production (62). The involvement of S100A9 in rainbow trout RBC response to VHSV infection has not been studied and will be part of our future investigations. PRDX, or natural killer enhancing factor (NKEF), belongs to a family of antioxidant enzymes that has been described to protect against viral infection in fish (63). In VHSV-exposed RBCs, increased *nkef* transcripts were detected at 3 and 72 hpe (4). However, further studies are needed to determine the role of fish RBC NKEF in VHSV infection. This is part of our ongoing research.

Also related to the antiviral immune response, we identified the IFIT5 protein in the IP proteomic analysis. IFITs are a family of proteins with tetratricopeptide repeats induced after the production of type I interferon (8). These proteins have recently emerged as important players in antiviral innate immunity (12–18). IFIT genes have been identified for many species, including mammals and various birds, reptiles, amphibians, and bony fish (9). Until now, a wide repertoire of mechanisms have proposed

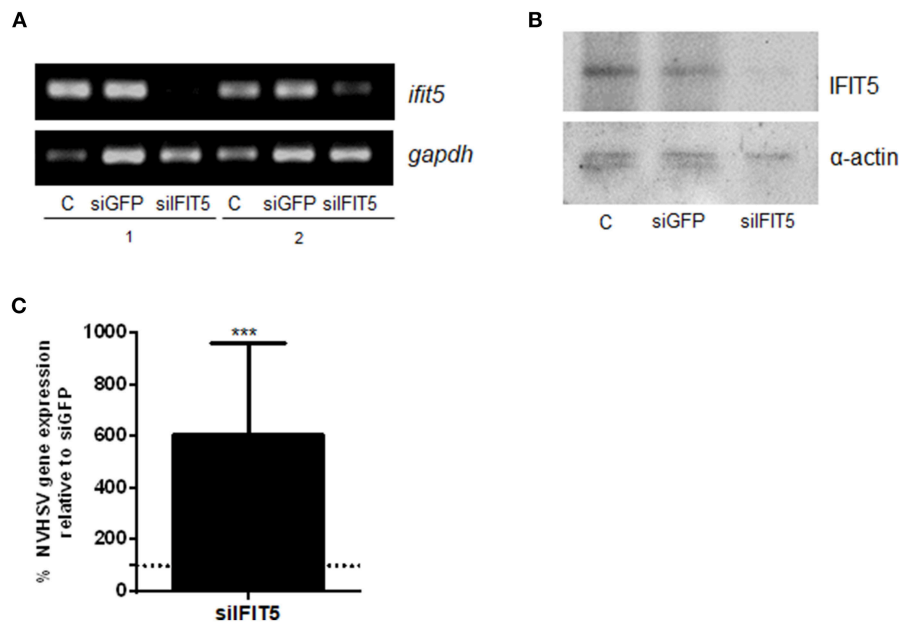


FIGURE 5 | The effect of *ifit5* silencing on VHSV replication. RBCs electroporated with a mixture of 3 different *ifit5* siRNA sequences were incubated for 3 days. **(A)** *ifit5* gene silencing was evaluated by RT-PCR. siGFP was used as a negative control. The endogenous gene control was *gapdh*. C shows RBCs electroporated without RNA; 1 and 2 indicate the sample number. **(B)** Representative image of IFIT5 silencing at protein level by western blot using anti-IFIT5 antibody. The endogenous protein control was α -actin. **(C)** At 3 days after siRNA treatment, RBCs were exposed to VHSV MOI 1 for 24 h. The percentage of VHSV replication relative to the negative control was evaluated by RT-qPCR of the NVHSV gene. Gene expression was normalized to the reference eukaryotic 18S rRNA gene. Data represent the mean \pm SD, $n = 3$. A Wilcoxon matched-pairs signed rank test was performed for statistical analysis. *** $P < 0.001$.

as to how IFIT proteins restrict viral replication (64). Here, we showed a correlation between decreasing VHSV replication and the highest IFIT5 expression at 6 hpe in RBCs. However, in RTG-2 cells exposed to VHSV, there was no correlation with decreasing viral replication as occurs in RBCs despite upregulation of *ifit5* gene expression. This may be due to the high constitutive *ifit5* gene expression level that we found in RBCs compared with RTG-2 (Supplementary Figure 4). Some untreated RBCs showed intense cell staining with IFIT5 antibody in immunofluorescence experiments, which may also result from the high constitutive *ifit5* expression level in RBCs. Similar to IFIT5, another interferon-stimulated gene (ISG) protein such as Mx was reported to have a high basal expression level in RBCs (7). Therefore, high IFIT5 basal levels could be implicated in the early disappearance of VHSV. IFIT5 expression was not affected by the reported decrease of type I IFN production after VHSV exposure (4). Therefore, IFIT5 expression could be independent of IFN production, as has been described with Mx mRNA expression in rainbow trout injected with a plasmid encoding the chemokine CK5B (65). Proteomic sequencing of rainbow trout RBCs transfected with a plasmid encoding GVHSV revealed upregulation of antiviral mechanisms by ISG15. This was validated by the upregulation of *mx*, *pkrr*, and *ifit5* gene expression, although *ifn1* gene expression appeared to be downregulated (40).

ifit5 silencing resulted in a significant increase in VHSV replication in RBCs. Similar results were found with the

generation of a chicken IFIT5 knockout fibroblast cell line by using the genome editing technology CRISPR/Cas9. Infection of this fibroblast IFIT5-ko cell line with RNA viruses such as Newcastle disease virus and VSV substantially supported viral replication in both cases (16). These results confirmed that IFIT5 is a crucial antiviral effector and that IFIT5 elimination weakens host barriers.

Mammalian IFIT5 also appears to have antiviral activity as an effector molecule by sequestration of viral RNA translation and through initiation of the innate immune response (66).

Upregulation of immune genes, such as *ifit5*, in Atlantic salmon after an intramuscular injection of IFN γ results in protection against ISAV infection (67). Thus, it is possible that fish IFIT5, an ortholog of mammalian IFIT5 (8), participates in antiviral mechanisms. The crystal structure of human IFIT5 shows a RNA-binding pocket cavity, which supports the antiviral mechanism of sequestering viral RNA and dampening translation (28). This mechanism is used by IFIT proteins to bind viral mRNA and subsequently restrict viral replication (14–16). Here we show that modulating IFIT5 activity in rainbow trout RBCs, by using a chemical compound obtained by *in silico* molecular docking or with VHSV RNA, resulted in increased VHSV replication. These results indicated that rainbow trout IFIT5 may mediate antiviral activity in RBCs by binding viral RNA to the IFIT5 RNA-binding pocket cavity, thereby decreasing viral replication. This represents the first report of a fish IFIT5 antiviral

mechanism. Similarly, chicken IFIT5 was recently described to specifically antagonize RNA viruses via this mechanism (16).

IFIT5 can also positively regulate innate immune responses in humans (13, 68, 69): ectopic expression of human IFIT5 upregulated the gene expression of IFN regulatory factor 3 (*irf3*) and nuclear factor- κ B (*nfk β*), whereas knockdown of IFIT5 impaired the transcription of these genes (68, 69). Nevertheless, non-significant differences were observed in the gene expression of Mx, IFN β , viperin, interferon-induced 35 kDa (IFI35), and Arf-GAP with dual PH domain-containing protein 2 (ADAP2) proteins between transgenic and non-transgenic chicken that constitutively and stably expressed IFIT5 (66). However, previous studies of VHSV-exposed RBCs have shown downregulation of IFN1 protein and basal levels of Mx protein but upregulation of the cytokines interleukin 1 β (IL1 β) and IL8, which are known to be activated by the transcription factor NF κ B (4). Therefore, an increase in these cytokines could be related to the NF κ B positive regulation by IFIT5. The role of rainbow trout IFIT5 in the activation of innate immune signaling pathways in RBCs needs to be further studied and is part of our ongoing research.

IFIT proteins can bind to viral proteins; for example, IFIT1 can bind to E1, a viral helicase of HPV, preventing viral replication in the nucleus (18). However, to our knowledge **it has not been reported whether IFIT5 can interact directly with viral proteins.** To this end, we investigated whether IFIT5 interacted with VHSV using a PLA. GVHSV protein was selected because it is the major virion surface protein and hence could increase the possibility of interaction with IFIT5. **We found a significant increase in IFIT5-GVHSV colocalization-positive cells in VHSV-exposed RBCs compared to unexposed RBCs.** More studies are needed to confirm an interaction between GVHSV and IFIT5, but it is clear that IFIT5 and VHSV are close enough to colocalize in the PLA.

In summary, **we identified host proteins in rainbow trout RBCs that immunoprecipitated with VHSV.** We focused on IFIT5 because it has recently emerged as an important player in antiviral innate immunity. We described a new defense mechanism based on IFIT5 antiviral activity in nucleated RBCs that appeared to contribute to halting the VHSV infection. This finding sheds light into novel antiviral therapeutics to mitigate the economic losses and social impact caused by viral infections in the aquaculture industry. This work broadens the knowledge of fish nucleated RBCs functions and their role in the immune response to viral infections.

REFERENCES

- Moras M, Lefevre SD, Ostuni MA. From erythroblasts to mature red blood cells: organelle clearance in mammals. *Front Physiol.* (2017) 8:1076. doi: 10.3389/fphys.2017.01076
- Glomski CA, Tamburlin J, Chainani M. The phylogenetic odyssey of the erythrocyte. III. fish, the lower vertebrate experience. *Histol Histopathol.* (1992) 7:501–28.
- Nombela I, Ortega-Villaizan MDM. Nucleated red blood cells: immune cell mediators of the antiviral response. *PLoS Pathog.* (2018) 14:e1006910. doi: 10.1371/journal.ppat.1006910
- Nombela I, Puente-Marin S, Chico V, Villena AJ, Carracedo B, Ciordia S, et al. Identification of diverse defense mechanisms in rainbow trout red blood cells in response to halted replication of VHS virus. *F1000Res.* (2017) 6:1958. doi: 10.12688/f1000research.12985.1
- Wessel O, Olsen CM, Rimstad E, Dahle MK. Piscine orthoreovirus (PRV) replicates in Atlantic salmon (*Salmo salar* L.) erythrocytes ex vivo. *Vet Res.* (2015) 46:26. doi: 10.1186/s13567-015-0154-7
- Workenhe ST, Wadowska DW, Wright GM, Kibenge MJ, Kibenge FS. Demonstration of infectious salmon anaemia virus (ISAV) endocytosis in erythrocytes of Atlantic salmon. *Virology J.* (2007) 4:13. doi: 10.1186/1743-422X-4-13

ETHICS STATEMENT

Experimental protocols and methods relating to experimental animals were reviewed and approved by the Animal Welfare Body and the Research Ethics Committee at the University Miguel Hernández (approval number 2014.205.E.OEP; 2016.221.E.OEP) and by the competent authority of the Regional Ministry of Presidency and Agriculture, Fisheries, Food and Water supply (approval number 2014/VSC/PEA/00205). All methods were carried out in accordance with the Spanish Royal Decree RD 53/2013 and EU Directive 2010/63/EU for the protection of animals used for research experimentation and other scientific purposes.

AUTHOR CONTRIBUTIONS

VC conceived ideas, performed experiments, analyzed data, and wrote the manuscript. MS-M and SP-M performed experiments. SC and MM performed proteomic sequencing. LM, IN, and FG produced antibodies. JE performed molecular docking analyses. MO-V conceived ideas, oversaw the research, analyzed data, and cowrote the manuscript. LP, JE, and JC contributed to the preparation of the manuscript.

FUNDING

This work was supported by the European Research Council (ERC Starting Grant GA639249).

ACKNOWLEDGMENTS

The authors would like to thank Remedios Torres and Efrén Lucas for their technical assistance. The proteomic analysis was performed in the Proteomics Facility of the Spanish National Center for Biotechnology (CNB-CSIC) belonging to ProteoRed, PRB3-ISCI, supported by grant PT17/0019. Thanks are also due to the three reviewers for their constructive comments and corrections.

SUPPLEMENTARY MATERIAL

The Supplementary Material for this article can be found online at: <https://www.frontiersin.org/articles/10.3389/fimmu.2019.00613/full#supplementary-material>

7. Nombela I, Carrion A, Puente-Marin S, Chico V, Mercado L, Perez L, et al. Infectious pancreatic necrosis virus triggers antiviral immune response in rainbow trout red blood cells, despite not being infective. *F1000Res*. (2017) 6:1968. doi: 10.12688/f1000research.12994.2
8. Zhou X, Michal JJ, Zhang L, Ding B, Lunney JK, Liu B, et al. Interferon induced IFIT family genes in host antiviral defense. *Int J Biol Sci*. (2013) 9:200–8. doi: 10.7150/ijbs.5613
9. Fensterl V, Sen GC. Interferon-induced Ifit proteins: their role in viral pathogenesis. *J Virol*. (2015) 89:2462–8. doi: 10.1128/JVI.02744-14
10. Varela M, Diaz-Rosales P, Pereiro P, Forn-Cuni G, Costa MM, Dios S, et al. Interferon-induced genes of the expanded IFIT family show conserved antiviral activities in non-mammalian species. *PLoS ONE*. (2014) 9:e100015. doi: 10.1371/journal.pone.0100015
11. D'Andrea LD, Regan L. TPR proteins: the versatile helix. *Trends Biochem Sci*. (2003) 28:655–62. doi: 10.1016/j.tibs.2003.10.007
12. Fensterl V, Sen GC. The ISG56/IFIT1 gene family. *J Interferon Cytokine Res*. (2011) 31:71–8. doi: 10.1089/jir.2010.0101
13. Diamond MS, Farzan M. The broad-spectrum antiviral functions of IFIT and IFITM proteins. *Nat Rev Immunol*. (2013) 13:46–57. doi: 10.1038/nri3344
14. Pichlmair A, Lassnig C, Eberle CA, Gorna MW, Baumann CL, Burkard TR, et al. IFIT1 is an antiviral protein that recognizes 5'-triphosphate RNA. *Nat Immunol*. (2011) 12:624–30. doi: 10.1038/ni.2048
15. Daffis S, Szretter KJ, Schriewer J, Li J, Youn S, Errett J, et al. 2'-O methylation of the viral mRNA cap evades host restriction by IFIT family members. *Nature*. (2010) 468:452–6. doi: 10.1038/nature09489
16. Santhakumar D, Rohaim M, Hussein HA, Hawes P, Ferreira HL, Behboudi S, et al. Chicken interferon-induced protein with tetratricopeptide repeats 5 antagonizes replication of RNA Viruses. *Sci Rep*. (2018) 8:6794. doi: 10.1038/s41598-018-24905-y
17. Hui DJ, Bhasker CR, Merrick WC, Sen GC. Viral stress-inducible protein p56 inhibits translation by blocking the interaction of eIF3 with the ternary complex eIF2.GTP.Met-tRNAi. *J Biol Chem*. (2003) 278:39477–82. doi: 10.1074/jbc.M305038200
18. Terenzi F, Saikia P, Sen GC. Interferon-inducible protein, P56, inhibits HPV DNA replication by binding to the viral protein E1. *EMBO J*. (2008) 27:3311–21. doi: 10.1038/emboj.2008.241
19. Banerjee P, Erehman J, Gohlke BO, Wilhelm T, Preissner R, Dunkel M. Super natural II—a database of natural products. *Nucleic Acids Res*. (2015) 43:D935–9. doi: 10.1093/nar/gku886
20. LeBerre M, De Kinkelin P, Metzger A. Identification sérologique des rhabdovirus des salmonidés. *Bull Office Int Epizooties*. (1977) 87:391–3.
21. Winton J, Batts W, deKinkelin P, LeBerre M, Bremont M, Fijan N. Current lineages of the epithelioma papulosum cyprini (EPC) cell line are contaminated with fathead minnow, *Pimephales promelas*, cells. *J Fish Dis*. (2010) 33:701–4. doi: 10.1111/j.1365-2761.2010.01165.x
22. Basurco B, Coll JM. Spanish isolates and reference strains of viral haemorrhagic septicaemia virus shown similar protein size patterns. *Bull Euro Assoc Fish Pathol*. (1989) 9:92–5.
23. Sanz F, Basurco B, Babin M, Dominguez J, Coll JM. Monoclonal antibodies against the structural proteins of viral haemorrhagic septicaemia virus isolates. *J Fish Dis*. (1993) 16:53–63. doi: 10.1111/j.1365-2761.1993.tb00847.x
24. Shevchenko A, Wilm M, Vorm O, Mann M. Mass spectrometric sequencing of proteins silver-stained polyacrylamide gels. *Anal Chem*. (1996) 68:850–8. doi: 10.1021/ac950914h
25. Puente-Marin S, Nombela I, Ciordia S, Mena MC, Chico V, Coll J, et al. *In Silico* functional networks identified in fish nucleated red blood cells by means of transcriptomic and Proteomic profiling. *Genes (Basel)*. (2018) 9:E202. doi: 10.3390/genes9040202
26. Szklarczyk D, Franceschini A, Wyder S, Forslund K, Heller D, Huerta-Cepas J, et al. STRING v10: protein-protein interaction networks, integrated over the tree of life. *Nucleic Acids Res*. (2015) 43:D447–52. doi: 10.1093/nar/gku1003
27. Houghten RA. General method for the rapid solid-phase synthesis of large numbers of peptides: specificity of antigen-antibody interaction at the level of individual amino acids. *Proc Natl Acad Sci USA*. (1985) 82:5131–5. doi: 10.1073/pnas.82.15.5131
28. Abbas YM, Pichlmair A, Gorna MW, Superti-Furga G, Nagar B. Structural basis for viral 5'-PPP-RNA recognition by human IFIT proteins. *Nature*. (2013) 494:60–4. doi: 10.1038/nature11783
29. Biasini M, Bienert S, Waterhouse A, Arnold K, Studer G, Schmidt T, et al. SWISS-MODEL: modelling protein tertiary and quaternary structure using evolutionary information. *Nucleic Acids Res*. (2014) 42:W252–8. doi: 10.1093/nar/gku340
30. Encinar JA, Fernandez-Ballester G, Galiano-Ibarra V, Micol V. *In silico* approach for the discovery of new PPARgamma modulators among plant-derived polyphenols. *Drug Des Devel Ther*. (2015) 9:5877–95. doi: 10.2147/DDDT.S93449
31. Ruiz-Torres V, Losada-Echeberria M, Herranz-Lopez M, Barrajón-Catalan E, Galiano V, Micol V, et al. New mammalian target of rapamycin (mTOR) modulators derived from natural product databases and marine extracts by using molecular docking techniques. *Mar Drugs*. (2018) 16:E385. doi: 10.3390/md16100385
32. Schymkowitz J, Borg J, Stricher F, Nys R, Rousseau F, Serrano L. The FoldX web server: an online force field. *Nucleic Acids Res*. (2005) 33:W382–8. doi: 10.1093/nar/gki387
33. Trott O, Olson AJ. AutoDock Vina: improving the speed and accuracy of docking with a new scoring function, efficient optimization, and multithreading. *J Comput Chem*. (2010) 31:455–61. doi: 10.1002/jcc.21334
34. Galiano V, Garcia-Valtanen P, Micol V, Encinar JA. Looking for inhibitors of the dengue virus NS5 RNA-dependent RNA-polymerase using a molecular docking approach. *Drug Des Devel Ther*. (2016) 10:3163–81. doi: 10.2147/DDDT.S117369
35. Sander T, Freyss J, von Korff M, Rufener C. DataWarrior: an open-source program for chemistry aware data visualization and analysis. *J Chem Inf Model*. (2015) 55:460–73. doi: 10.1021/ci500588j
36. Lipinski CA, Lombardo F, Dominy BW, Feeney PJ. Experimental and computational approaches to estimate solubility and permeability in drug discovery and development settings. *Adv Drug Deliv Rev*. (2001) 46:3–26. doi: 10.1016/S0169-409X(00)00129-0
37. Cheng F, Li W, Zhou Y, Shen J, Wu Z, Liu G, et al. admetSAR: a comprehensive source and free tool for assessment of chemical ADMET properties. *J Chem Inf Model*. (2012) 52:3099–105. doi: 10.1021/ci300367a
38. Chico V, Gomez N, Estepa A, Perez L. Rapid detection and quantitation of viral hemorrhagic septicemia virus in experimentally challenged rainbow trout by real-time RT-PCR. *J Virol Methods*. (2006) 132:154–9. doi: 10.1016/j.jviromet.2005.10.005
39. Wang T, Johnson N, Zou J, Bols N, Secombes CJ. Sequencing and expression of the second allele of the interleukin-1beta gene in rainbow trout (*Oncorhynchus mykiss*): identification of a novel SINE in the third intron. *Fish Shellfish Immunol*. (2004) 16:335–58. doi: 10.1016/S1050-4648(03)00114-1
40. Puente-Marin S, Nombela I, Chico V, Ciordia S, Mena M, Coll J, et al. Rainbow trout erythrocytes ex vivo transfection with a DNA vaccine encoding VHSV glycoprotein G induces an antiviral immune response. *Front Immunol*. (2018) 9:2477. doi: 10.3389/fimmu.2018.02477
41. Raida MK, Buchmann K. Temperature-dependent expression of immune-relevant genes in rainbow trout following *Yersinia ruckeri* vaccination. *Dis Aquat Organ*. (2007) 77:41–52. doi: 10.3354/dao01808
42. Blanchard EL, Loomis KH, Bhosle SM, Vanover D, Baumhof P, Pitard B, et al. Proximity ligation assays for *in situ* detection of innate immune activation: focus on *in vitro*-transcribed mRNA. *Mol Ther Nucleic Acids*. (2018) 14:52–66. doi: 10.1016/j.omtn.2018.11.002
43. Assenberg R, Delmas O, Morin B, Graham SC, De Lamballerie X, Laubert C, et al. Genomics and structure/function studies of Rhabdoviridae proteins involved in replication and transcription. *Antiviral Res*. (2010) 87:149–61. doi: 10.1016/j.antiviral.2010.02.322
44. Salentin S, Schreiber S, Haupt VJ, Adasme MF, Schroeder M. PLIP: fully automated protein-ligand interaction profiler. *Nucleic Acids Res*. (2015) 43:W443–7. doi: 10.1093/nar/gkv315
45. Cervantes-Salazar M, Angel-Ambrocio AH, Soto-Acosta R, Bautista-Carbajal P, Hurtado-Monzon AM, Alcaraz-Estrada SL, et al. Dengue virus NS1 protein interacts with the ribosomal protein RPL18: this interaction is required for viral translation and replication in Huh-7 cells. *Virology*. (2015) 484:113–26. doi: 10.1016/j.virol.2015.05.017
46. Bee A, Ke Y, Forootan S, Lin K, Beesley C, Forrest SE, et al. Ribosomal protein l19 is a prognostic marker for human prostate cancer. *Clin Cancer Res*. (2006) 12(7 Pt 1):2061–5. doi: 10.1158/1078-0432.CCR-05-2445

47. Lindstrom MS. Emerging functions of ribosomal proteins in gene-specific transcription and translation. *Biochem Biophys Res Commun.* (2009) 379:167–70. doi: 10.1016/j.bbrc.2008.12.083
48. Chen FW, Ioannou YA. Ribosomal proteins in cell proliferation and apoptosis. *Int Rev Immunol.* (1999) 18:429–48. doi: 10.3109/08830189909088492
49. Liu XY, Li GQ, Ma Y, Zhao LJ. Topological centrality-based identification of hub genes and pathways associated with acute viral respiratory infection in infants. *Genet Mol Res.* (2015) 14:18334–43. doi: 10.4238/2015.December.23.21
50. Le Sommer C, Barrows NJ, Bradrick SS, Pearson JL, Garcia-Blanco MA. G protein-coupled receptor kinase 2 promotes flaviviridae entry and replication. *PLoS Negl Trop Dis.* (2012) 6:e1820. doi: 10.1371/journal.pntd.0001820
51. Yuhashi K, Ohnishi S, Kodama T, Koike K, Kanamori H. *In vitro* selection of the 3'-untranslated regions of the human liver mRNA that bind to the HCV nonstructural protein 5B. *Virology.* (2014) 450–451:13–23. doi: 10.1016/j.virol.2013.11.036
52. Lee AS, Burdeinick-Kerr R, Whelan SP. A ribosome-specialized translation initiation pathway is required for cap-dependent translation of vesicular stomatitis virus mRNAs. *Proc Natl Acad Sci USA.* (2013) 110:324–9. doi: 10.1073/pnas.1216454109
53. Yang SH, Liu ML, Tien CF, Chou SJ, Chang RY. Glyceraldehyde-3-phosphate dehydrogenase (GAPDH) interaction with 3' ends of Japanese encephalitis virus RNA and colocalization with the viral NS5 protein. *J Biomed Sci.* (2009) 16:40. doi: 10.1186/1423-0127-16-40
54. Kishimoto N, Onitsuka A, Kido K, Takamune N, Shoji S, Misumi S. Glyceraldehyde 3-phosphate dehydrogenase negatively regulates human immunodeficiency virus type 1 infection. *Retrovirology.* (2012) 9:107. doi: 10.1186/1742-4690-9-107
55. Kishimoto N, Onitsuka-Kishimoto A, Iga N, Takamune N, Shoji S, Misumi S. The C-terminal domain of glyceraldehyde 3-phosphate dehydrogenase plays an important role in suppression of tRNA(Lys3) packaging into human immunodeficiency virus type-1 particles. *Biochem Biophys Rep.* (2016) 8:325–32. doi: 10.1016/j.bbrep.2016.09.015
56. Chaturvedi S, Seo JK, Rao AL. Functionality of host proteins in cucumber mosaic virus replication: GAPDH is obligatory to promote interaction between replication-associated proteins. *Virology.* (2016) 494:47–55. doi: 10.1016/j.virol.2016.04.001
57. Allonso D, Andrade IS, Conde JN, Coelho DR, Rocha DC, da Silva ML, et al. Dengue virus NS1 protein modulates cellular energy metabolism by increasing glyceraldehyde-3-phosphate dehydrogenase activity. *J Virol.* (2015) 89:11871–83. doi: 10.1128/JVI.01342-15
58. Prasanth KR, Huang YW, Liou MR, Wang RY, Hu CC, Tsai CH, et al. Glyceraldehyde 3-phosphate dehydrogenase negatively regulates the replication of bamboo mosaic virus and its associated satellite RNA. *J Virol.* (2011) 85:8829–40. doi: 10.1128/JVI.00556-11
59. Dollenmaier G, Weitz M. Interaction of glyceraldehyde-3-phosphate dehydrogenase with secondary and tertiary RNA structural elements of the hepatitis A virus 3' translated and non-translated regions. *J Gen Virol.* (2003) 84(Pt 2):403–14. doi: 10.1099/vir.0.18501-0
60. De BP, Gupta S, Zhao H, Drazba JA, Banerjee AK. Specific interaction *in vitro* and *in vivo* of glyceraldehyde-3-phosphate dehydrogenase and LA protein with cis-acting RNAs of human parainfluenza virus type 3. *J Biol Chem.* (1996) 271:24728–35. doi: 10.1074/jbc.271.40.24728
61. Wu R, Zhang Y, Xiang Y, Tang Y, Cui F, Cao J, et al. Association between serum S100A9 levels and liver necroinflammation in chronic hepatitis B. *J Transl Med.* (2018) 16:83. doi: 10.1186/s12967-018-1462-2
62. Darweesh MF, Rajput MKS, Braun LJ, Rohila JS, Chase CCL. BVDV Npro protein mediates the BVDV induced immunosuppression through interaction with cellular S100A9 protein. *Microb Pathog.* (2018) 121:341–9. doi: 10.1016/j.micpath.2018.05.047
63. Valero Y, Martinez-Morcillo FJ, Esteban MA, Chaves-Pozo E, Cuesta A. Fish peroxiredoxins and their role in immunity. *Biology (Basel).* (2015) 4:860–80. doi: 10.3390/biology4040860
64. Vladimer GI, Gorna MW, Superti-Furga G. IFITs: emerging roles as key anti-viral proteins. *Front Immunol.* (2014) 5:94. doi: 10.3389/fimmu.2014.00094
65. Montero J, Chaves-Pozo E, Cuesta A, Tafalla C. Immune effects observed after the injection of plasmids coding for rainbow trout (*Oncorhynchus mykiss*) CK5B, CK6 and CK7A chemokines demonstrate their immunomodulatory capacity and reveal CK6 as a major interferon inducer. *Dev Comp Immunol.* (2009) 33:1137–45. doi: 10.1016/j.dci.2009.06.008
66. Rohaim MA, Santhakumar D, Naggat RFE, Iqbal M, Hussein HA, Munir M. Chickens Expressing IFIT5 ameliorate clinical outcome and pathology of highly pathogenic avian influenza and velogenic newcastle disease viruses. *Front Immunol.* (2018) 9:2025. doi: 10.3389/fimmu.2018.02025
67. Chang CJ, Robertsen C, Sun B, Robertsen B. Protection of Atlantic salmon against virus infection by intramuscular injection of IFN γ expression plasmid. *Vaccine.* (2014) 32:4695–702. doi: 10.1016/j.vaccine.2014.05.059
68. Zhang B, Liu X, Chen W, Chen L. IFIT5 potentiates anti-viral response through enhancing innate immune signaling pathways. *Acta Biochim Biophys Sin (Shanghai).* (2013) 45:867–74. doi: 10.1093/abbs/gmt088
69. Zheng C, Zheng Z, Zhang Z, Meng J, Liu Y, Ke X, et al. IFIT5 positively regulates NF- κ B signaling through synergizing the recruitment of IkappaB kinase (IKK) to TGF-beta-activated kinase 1 (TAK1). *Cell Signal.* (2015) 27:2343–54. doi: 10.1016/j.cellsig.2015.08.018

Conflict of Interest Statement: The authors declare that the research was conducted in the absence of any commercial or financial relationships that could be construed as a potential conflict of interest.

Copyright © 2019 Chico, Salvador-Mira, Nombela, Puente-Marin, Ciordia, Mena, Perez, Coll, Guzman, Encinar, Mercado and Ortega-Villaizan. This is an open-access article distributed under the terms of the Creative Commons Attribution License (CC BY). The use, distribution or reproduction in other forums is permitted, provided the original author(s) and the copyright owner(s) are credited and that the original publication in this journal is cited, in accordance with accepted academic practice. No use, distribution or reproduction is permitted which does not comply with these terms.